Laterally Modulated 2D Electron System in the Extreme Quantum Limit

S. Melinte,[1] Mona Berciu,[2,*] Chenggang Zhou,[1] E. Tutuc,[1] S. J. Papadakis,[1] C. Harrison,[3] E. P. De Poortere,[1]
Mingshaw Wu,[3] P. M. Chaikin,[3] M. Shayegan,[1] R. N. Bhatt,[1] and R. A. Register[4]

[1]*Department of Electrical Engineering, Princeton University, Princeton, New Jersey 08544, USA*
[2]*Department of Physics and Astronomy, University of British Columbia, Vancouver, British Columbia, Canada V6T 1Z1*
[3]*Department of Physics, Princeton University, Princeton, New Jersey 08544, USA*
[4]*Department of Chemical Engineering, Princeton University, Princeton, New Jersey 08544, USA*
(Received 27 May 2003; published 21 January 2004)

We report on magnetotransport of a two-dimensional electron system (2DES), located 32 nm below
the surface, with a surface superlattice gate structure of periodicity 39 nm imposing a periodic
modulation of its potential. For low Landau level fillings ν, the diagonal resistivity displays a rich
pattern of fluctuations, even though the disorder dominates over the periodic modulation. Theoretical
arguments based on the combined effects of the long-wavelength, strong disorder and the short-
wavelength, weak periodic modulation present in the 2DES qualitatively explain the data.

Two-dimensional electron systems (2DESs) subjected
to both an artificial periodic modulation and a quantizing,
perpendicular magnetic field B are expected to exhibit
remarkable behavior arising from the interplay of the
period of the modulation and the magnetic length, and
the relative strengths of the periodic modulation, cyclo-
tron energy ($\hbar\omega_c$), and disorder potential [1–3]. When the
periodic modulation's strength is weak compared to $\hbar\omega_c$,
each of the highly degenerate Landau levels (LLs) evolve
into an energy spectrum with recursive properties, the so-
called Hofstadter butterfly. In this limit, the structure of
the butterfly is controlled by the ratio of the magnetic flux
through the unit cell area $\mathcal{A}$ of the periodic modulation,
$\Phi = B\mathcal{A}$, to the flux quantum $\Phi_0 = h/e$. Optimally,
Φ/Φ_0 should be of order unity and B should be large
so that well-separated LLs are formed. This poses the
stringent requirement of a small unit cell area $\mathcal{A}$.
Additionally, the disorder, present in any real system,
should be small compared to the strength of the periodic
potential, so that the butterfly's larger energy gaps remain
open. Then, one may probe directly the effects of the
periodic modulation within a single, resolved LL. In
particular, maxima and minima are expected in the
low-temperature (T) diagonal resistivity ρ_{xx} as B is swept
at fixed density n through a LL, i.e., as the Fermi level
(E_F) moves through the subbands and subgaps of the
butterfly. Yet, for realistic disorder-broadened LLs, new
physics can occur, due to the competition between the
strengths of the disorder and the periodic modulation.

Here we present low-T magnetotransport measure-
ments in a GaAs/AlGaAs 2DES, at a distance of 32 nm
below the surface, whose potential is modulated via a
surface gate with triangular symmetry and a periodicity
of 39 nm, the smallest periodicity yet reported [4–6].
Moreover, our data are taken in the extreme quantum
limit, i.e., at low LL fillings ν where the integer quantum
Hall effect (QHE) [7] is observed. Despite the high qual-
ity of the 2DES and its close proximity to the modulating

gate [8], the disorder induced by doping impurities, lo-
cated at a distance of ≈ 20 nm, is much larger than the
periodic potential. Naively, one may expect that in this
regime where the periodic potential is only a small
perturbation, it should play no significant role in the
transport properties of the system. Surprisingly, our re-
sults reveal that the small periodic potential does play a
large role. Experimentally, we observe that the lowest
spin-down LL is significantly broadened and ρ_{xx} at
low ν exhibits a rich fluctuation pattern. Our theoretical
arguments, based on the combined effects of the weak,
short-wavelength periodic potential and the strong, long-
wavelength disorder, qualitatively explain the data. The
results highlight the importance of the very different
length scales of the disorder and the periodic potentials
in determining transport through the 2DES: because
there are large areas of the sample where the disorder
potential is very flat, the periodic potential plays the
dominant role locally—this is one of the rare cases in
physics where a small perturbation has a significant and
nontrivial effect.

The sample studied here was grown by molecular beam
epitaxy, and consists of a GaAs/Al$_{0.3}$Ga$_{0.7}$As heterostruc-
ture with a 2DES ($n \approx 3 \times 10^{11}$ cm^{-2}) at a distance $d =
32$ nm below the surface. The Si dopant atoms were
deposited at a distance of about 12 nm below the surface.
The low-T mobility, prior to and after the patterning, is
about 3×10^5 cm^2/V s. Experiments were performed on
20 μm-wide Hall bars fabricated by standard photoli-
thography and wet etching. The distance between the
probes used to measure the resistivity was 20 μm. The
resistivity coefficients [9] were measured by probe pairs
located in different regions of the Hall bar, yielding
qualitatively similar results. The 2DES is placed in a
periodic potential created by a top gate realized by means
of a diblock copolymer nanolithography technique [10].
First, a self-assembled layer of hexagonally ordered poly-
isoprene nanodomains (spheres with center-to-center

distance a) contained in a polystyrene matrix was formed on the sample's surface. After the removal of the polyisoprene spheres a polystyrene mask ≈ 15 nm thick is left on the surface and acts as a template for a Ti/Au metallic gate, whose potential V_g can be varied [see right inset of Fig. 1(a)]. Even without applying an external gate bias, a rich structure is present in the ρ_{xx} data for the patterned sample. This observation corroborates with the results of previous experiments [5,6] and theoretical calculations [11] which explain the modulation at zero bias through the effects of strain and Fermi level pinning at the semiconductor-metal (gate) interface.

The central result of our experimental work is shown in Fig. 1 where ρ_{xx} is displayed in the filling factor range $1.1 < \nu < 1.8$ at various temperatures for the patterned and unpatterned samples [9]. Several features of the data are noteworthy. (1) For both samples, ρ_{xx} exhibits a maximum centered around $\nu = 3/2$ and shows reproducible fluctuations at low T [12]. For the modulated sample, however, the observed fluctuations in ρ_{xx} are much stronger. Qualitatively similar data were reported in Ref. [4] for a similar device with 60 nm periodicity, giving further evidence that these fluctuations are intrinsic. (2) Compared to the data taken in the unpatterned sample, ρ_{xx} is dramatically distorted in the patterned sample and has an extended tail on the low-ν side. To
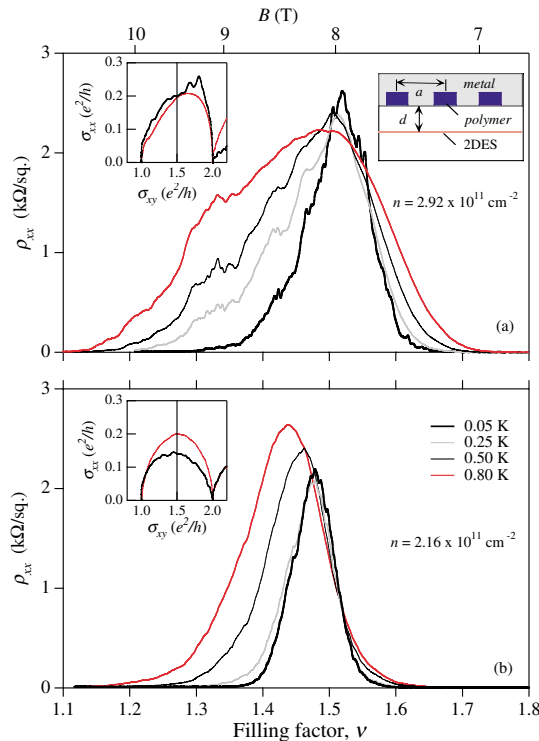
better illustrate the observed asymmetry for the patterned sample, we display in the insets of Fig. 1 the σ_{xx}, σ_{xy} flow diagram [7,9]. We note that both the ρ_{xx} fluctuations and the asymmetry are reproducible with repeating B sweeps and also varying T in the low-temperature range. (3) As T is raised, concomitantly with the weakening of the $\nu = 1$ QHE minimum, new peaks develop, growing out from the $\rho_{xx} = 0$ background. The peak near $\nu = 3/2$ broadens with increasing temperature and displays at $T = 0.80$ K a full width at half maximum (FWHM) up to 4 times larger than the low-T, saturated FWHM. In contrast, the FWHM in the unpatterned sample increases only by a factor of 2 for the same T range. (4) As seen in Fig. 2, where we present our lowest temperature ρ_{xx} as a function of ν for various gate voltages, the fluctuations appear predominantly on the low-ν side of the peak, regardless of the sign of V_g.

We now discuss the properties of the Hofstadter spectrum for parameters relevant to our sample. In the absence of disorder, and neglecting LL mixing, the electronic structure is a function only of the ratio Φ/Φ_0. For $\Phi/\Phi_0 = q/p$, with p and q mutually prime integers, the Landau band splits into q subbands. The Hofstadter butterfly for a repulsive ($V_1 > 0$) weak triangular modulation $V(x, y) = 2V_1\{\cos[\frac{2\pi}{a\sqrt{3}}(x + \sqrt{3}y)]+$ $\cos[\frac{2\pi}{a\sqrt{3}}(x - \sqrt{3}y)] + \cos(\frac{4\pi}{a\sqrt{3}}x)\}$ is shown in Fig. 3. The energies of the eigenstates are referenced to the lowest LL energy $\hbar\omega_c/2$ and are scaled by the amplitude of the first Fourier component of the periodic potential V_1 [2]. While the number of total subbands q jumps discontinuously as B is varied, from Fig. 3 it is apparent that for all $\Phi/\Phi_0 \in (m, m + 1)$, where m is an integer, the butterfly has precisely $m + 1$ main subbands, each of which has a fractal structure of its own. Simple arguments show that the total number of states per unit area in each of the upper m main subbands is $n_0 = 1/\mathcal{A}$, whereas the lowest main subband
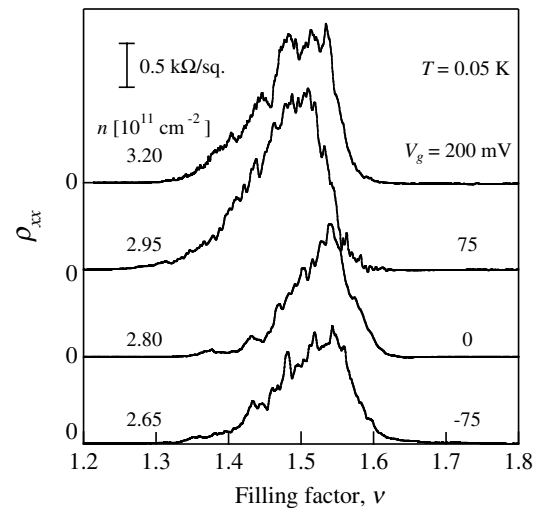

FIG. 1 (color online). ρ_{xx} vs ν traces for (a) the patterned sample at $V_g = 0$ V and (b) unpatterned sample at indicated temperatures. The top magnetic field scale is for the data of (a). Left insets: σ_{xx} (longitudinal) vs σ_{xy} (transversal conductivity) at $T = 0.05$ and 0.80 K. Right inset: side view of the device.

FIG. 2. ρ_{xx} vs ν at $T = 0.05$ K and various V_g (n). Curves for $V_g = 0$, 75, and 200 mV have been shifted for clarity.
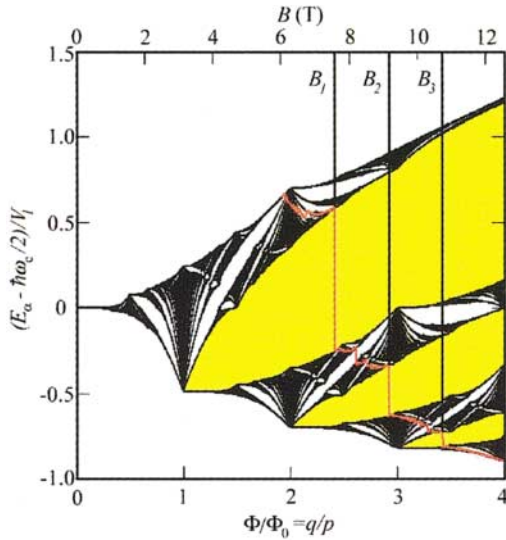
FIG. 3 (color).   Hofstadter butterfly of the spin-down lowest LL for a weak, repulsive, triangular potential modulation. The eigenenergies are plotted vs q/p, for p and q between 1 and 150. The position of E_F is shown by the red curve.

contains the rest of $[\Phi/(m\Phi_0) - 1]n_0$ states of the LL [13]. The three subgaps shown as yellow regions in Fig. 3 are the most robust against disorder: if disorder is small, one expects to see minima in ρ_{xx} when E_F is inside these subgaps ($\rho_{xx} \propto \sigma_{xx}$, [9]). For a given n we find the magnetic field B_i at which E_F is inside each of the main subgaps of the spin-down lowest LL to be $B_i = \Phi_0/2(n + in_0)$. For $n = 2.92 \times 10^{11}$ cm^{-2} ($V_g = 0$ in Fig. 1), E_F should cross the main subgaps at $B_1 = 7.6$ T, $B_2 = 9.2$ T, and $B_3 = 10.7$ T ($\nu = 1.59$, 1.31, and 1.13). Figures 1 and 2 show that the low-T ρ_{xx} vanishes for all $\nu \lesssim 1.3$ and $\nu \gtrsim 1.6$, suggesting that all states, except for a few in the second highest subband, are fully localized. The same conclusion is reached if the analysis is repeated for an attractive potential $V_1 < 0$, for which the Hofstadter structure of Fig. 3 is inverted.

These observations indicate that disorder plays an important role. From the measured low-T mobility we estimate the width of the disorder-broadened LLs at $0.24 \times (B[\mathrm{T}])^{1/2}$ meV [3]. For $B = 10$ T it is $\approx$ 0.7 meV, much larger than $V_1 = 0.1$ meV/V $\times V_g$(V) inferred from the exponentially decaying solution of the Laplace equation [8]. Although the modulation amplitude is not precisely known [11], in our sample it likely remains smaller than the disorder. Since the main subgaps are filled in by disorder, the features in ρ_{xx} (σ_{xx}) cannot be attributed to E_F crossing the smaller gaps inside the second subband (from B_1 to B_2); these smaller gaps must also be filled in by disorder. Hence, an interpretation of our data based on the naive Hofstadter butterfly is inappropriate.

In order to understand the origin of the ρ_{xx} features, we must analyze the new regime of a small periodic modulation and large disorder. Slowly varying disorder (ex-

pected in high-mobility, remotely doped samples such as ours) can be treated in semiclassical terms, with wave functions following the equipotentials of the disorder. The LLs are broadened, with all high (low) energy states being localized near maxima (minima) of the disorder potential. Current-carrying extended states correspond to equipotential contours percolated across the sample and are found in a so-called critical region at the center of the Landau band [7]. The effect of a supplementary weak periodic potential is illustrated in Fig. 4, where we plot equipotential contours of the total 2DES potential. The disorder potential is a sum of screened Coulomb potentials from doping impurities located 20 nm from the 2DES [14]. The amplitude of both disorder and the periodic potentials are close to experimental estimations. Instead of smooth trajectories, the equipotential contours now have a fractured nature, with many little "bubbles" around minima of the periodic potential on the flat areas of the disorder potential. Since the lattice constant a is comparable to the magnetic length, *quantum mechanical tunneling spreads the electronic wave functions over these flat regions, and considerably helps their percolation throughout the sample.* This picture is in qualitative agreement with the results of Figs. 1 and 2, which show that ρ_{xx} of the patterned sample is considerably enhanced with increasing T on the low-ν side, suggesting transport through temperature-activated hopping between nearby states, absent in the unpatterned sample.

This picture also offers a possible explanation for the detailed peak and valley structure observed in our magnetotransport data. Consider the area enclosed in the rectangle drawn in Fig. 4, which is almost disorder-free
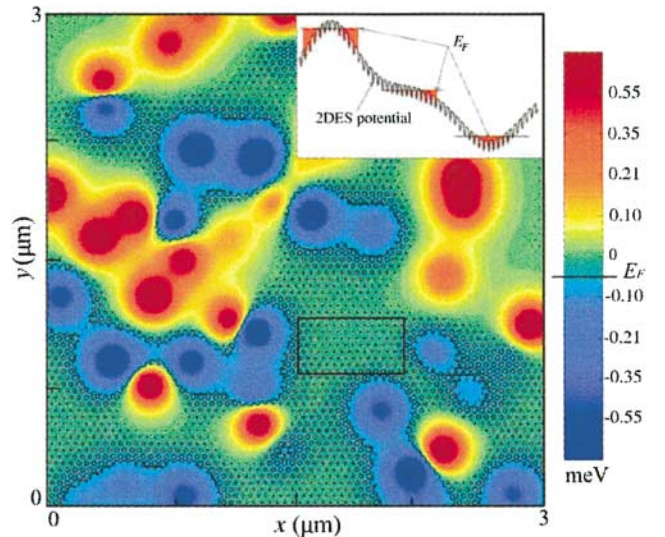

FIG. 4 (color).   The equipotential contours (black curves) of the total 2DES potential at $\nu = 1.3$. The 2DES potential consists of a weak, attractive, triangular periodic modulation and a slowly varying disorder potential. Minima (maxima) of the disorder potential are shown in blue (red). The inset schematically shows E_F crossing through the 2DES potential.
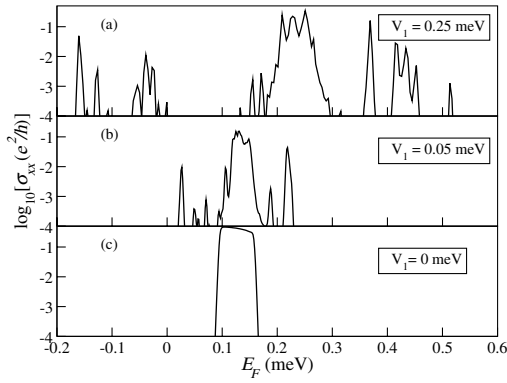
FIG. 5. σ_{xx} vs E_F for a 3.1×2.9 μm^2 sample at $T = 0.01$ K and indicated V_1 for $q/p = 5/2$. The standard deviation of the disorder potential is 0.7 meV. E_F is measured from $\hbar\omega_c/2$.

(it has very little underlying disorder variation). Wave functions across such flat regions correspond to those of finite-area Hofstadter butterflies, with appropriate boundary conditions. For the appropriate energy range, E_F is inside either a subband or a gap of such local Hofstadter structures. If E_F is inside a subband, wave functions span the flat region and help enhance the percolation. When E_F is inside a gap, there are no states supported by the flat region and, hence, no current can flow across it. Such flat regions act as switches which are turned on or off as E_F is changed, helping or hindering the current flow through the sample. When one or more switches are off, there are fewer paths for the current to be carried across the sample, and a valley is expected in σ_{xx} (ρ_{xx}).

Finally, the appearance of the fluctuation pattern preponderantly on the low-ν side (see Fig. 2) is a direct consequence of the particle-hole asymmetry of the triangular potential. For LL filling factors $1 < \nu < 3/2$ ($3/2 < \nu < 2$), percolation between wave functions localized around minima (maxima) of the disorder is helped by the bubbles centered on the minima (maxima) of the periodic potential (see inset of Fig. 4). When attractive, the triangular potential has deep minima on a triangular pattern, and shallow maxima on a displaced honeycomb pattern (notice that there are almost no honeycomb arranged bubbles in Fig. 4). For $3/2 < \nu < 2$, the shallow maxima of the periodic potential are not as effective in enhancing percolation, and σ_{xx} (ρ_{xx}) in the modulated sample is similar to that of the unpatterned sample.

These semiclassical arguments are supported by preliminary computations of σ_{xx}, shown in Fig. 5, based on the Kubo-Landauer formalism [14]. The calculation is done for a given realization of a slowly varying disorder potential and for a fixed value of B. As n is varied from 2.6×10^{11} cm^{-2} to 3.4×10^{11} cm^{-2}, E_F sweeps through the disorder-broadened LL. In Fig. 5(a), the peak-to-peak amplitude of the periodic modulation—$9V_1$ for the triangular superlattice—is somewhat larger than disorder's strength. Well-defined subbands start to separate and evolve towards the Hofstadter butterfly structure ex-

pected in the limit where disorder becomes negligible compared to the periodic modulation. In the opposite limit of no periodic modulation [Fig. 5(c)], we observe a narrow, smooth peak when E_F is inside the critical region of percolated states (not centered at $E = 0$ because the disorder potential is not particle-hole symmetric). For a periodic modulation weaker or comparable to the disorder strength [Fig. 5(b)], a pattern of peaks and valleys emerges, as the periodic potential influences the percolation inside and near the critical region. Efforts to improve the description of the disorder potential are under way, so that quantitative comparisons with the experiment become possible.

To conclude, our work extends the rich problem of modulated 2DESs in quantizing magnetic fields to a new regime of long-wavelength, strong disorder and short-wavelength, weak periodic potential, and uncovers yet more interesting physics.

---

*Corresponding author.
 Email address: berciu@physics.ubc.ca
[1] D. R. Hofstadter, Phys. Rev. B **14**, 2239 (1976).
[2] F. H. Claro and G. H. Wannier, Phys. Rev. B **19**, 6068 (1979).
[3] D. Pfannkuche and R. R. Gerhardts, Phys. Rev. B **46**, 12 606 (1992).
[4] C. G. Smith *et al.*, J. Vac. Sci. Technol. B **10**, 2904 (1992).
[5] T. Schlösser *et al.*, Europhys. Lett. **33**, 683 (1996).
[6] C. Albrecht *et al.*, Phys. Rev. Lett. **86**, 147 (2001).
[7] *The Quantum Hall Effect*, edited by R. E. Prange and S. M. Girvin (Springer-Verlag, New York, 1987).
[8] The potential modulation seen by the 2DES is equal to the modulation of the periodic gate potential, attenuated by the factor $\exp(-4\pi d/\sqrt{3}a)$. A low attenuation requires a large a/d ratio, which highlights the critical role of high quality *shallow* 2DESs for the experiments.
[9] The longitudinal and transverse resistivities ρ_{xx} and ρ_{xy} were recorded at both positive and negative B to eliminate the mixing between transport tensor components. σ_{xx} and σ_{xy} were then determined from the standard relations $\sigma_{xx} = \rho_{xx}/(\rho_{xx}^2 + \rho_{xy}^2)$; $\sigma_{xy} = \rho_{xy}/(\rho_{xx}^2 + \rho_{xy}^2)$.
[10] C. Harrison *et al.*, J. Vac. Sci. Technol. B **16**, 544 (1998).
[11] J. H. Davies and I. A. Larkin, Phys. Rev. B **49**, 4800 (1994).
[12] Several studies on narrow, quasi-one-dimensional channels have revealed the presence of fluctuations in transport coefficients, predominantly near the breakdown of the QHE [J. A. Simmons *et al.*, Phys. Rev. Lett. **63**, 1731 (1989)]. The conduction mechanism in these narrow samples is consistent with the model of tunneling-assisted percolation between opposite edge states [J. K. Jain and S. A. Kivelson, Phys. Rev. Lett. **60**, 1542 (1988)].
[13] These values lead to the correct Chern numbers.
[14] C. Zhou, M. Berciu, and R. N. Bhatt (unpublished).